

14. R. W. Lenz, C. C. Han, J. Stenger-Smith, and F. E. Karasz, *J. Polym. Sci., Polym. Chem. Ed.*, **26**, 3241, (1988).
 15. I. Murase, T. Ohnishi, T. Noguchi, and M. Hirooka, *Polym. Commun.*, **28**, 229, (1987).
 16. J. I. Jin, S. H. Yu, and H. K. Shim, *J. Polym. Sci., Polym. Chem.*, in press, 1992.
 17. S. K. Kim, Diploma thesis, Korea University, Seoul (1988).

Theoretical Investigation of the Vibrational Relaxation of NO($v=1-7$) in Collisions with O₂ and N₂

Jongbaik Ree

Department of Chemistry, College of Education, Chonnam National University,
 Kwangju 500-757. Received July 20, 1992

The vibrational relaxation rate constants of NO($v=1-7$) by O₂ and N₂ have been calculated in the temperature range of 300-1000 K using the solution of the time-dependent Schrödinger equation. The calculated relaxation rate constants by O₂ increase monotonically with the vibrational energy level v , which is compatible with the experimental data, while those by N₂ are nearly independent of v in the range of $3.40 \pm 1.60 \times 10^{-16}$ cm³/molecule-sec at 300 K. Those for NO(v)+N₂ are about 2-3 orders of magnitude smaller than those for NO(v)+O₂, because the latter is an exothermic processes while the former an endothermic. Relaxation processes can be interpreted by single-quantum V-V transition. The contributions of V-T/R transition and double-quantum V-V transition to the relaxation are negligible over the entire temperature range.

Introduction

Nitric oxide is a prominent infrared radiator in the ionosphere. Its vibrational energy transfer rate with atmospheric species is necessary to describe properly nonequilibrium infrared radiative phenomena in the excited atmosphere. In particular, quenching of vibrationally excited NO by O₂, N₂, and O in the upper atmosphere is of great significance. The vibrational relaxation of nitric oxide through collisions with atoms, diatomic and simple polyatomic molecules have been extensively studied over wide temperature ranges.¹⁻¹² There have been several measurements of the relaxation rates of the first excited vibrational level of NO in the X²I state by O₂ and N₂, and the rate constants for these processes are well established.⁴⁻⁶

However, little has been known on the relaxation of vibrational levels $v>1$ for these collision systems. Murphy *et al.* mentioned⁴ that "Based on the assumption that quenching of NO(v) by O₂ is proportional to v , the quenching rate constant obtained for NO($v=1$) by O₂ is $2.4 \pm 1.5 \times 10^{-14}$ cm³/sec. If the quenching of NO(v) by O₂ is independent of v , the reported rate constant is increased by 75%. The quenching rate of NO($v=1$) by N₂ obtained is $1.7 \pm 0.7 \times 10^{-16}$ cm³/sec where the uncertainty includes both the quenching models proportional and independent of v ." Using Lambert-Salter probability scaling for $v=1$ and their experimental data, Whitson, Darnton, and McNeal⁷ have placed the bounds on the rate coefficients of the processes NO(v)+O₂→NO($v-1$)+O₂ for $v=1-7$. Their reduced scaling is sub-linear with v . Green *et al.*⁸ have also determined the room temperature rate coefficients for the above process for $v=1-7$, and have found that the rate coefficient increases monotonically with

v . To our knowledge, however, the vibrational relaxation rate of NO(v) by N₂ for $v>1$ has never been reported.

The present study was aimed to calculate the vibrational relaxation of NO($v=1-7$) by O₂ and N₂ through a semiclassical procedure. In this collision system, the vibrational relaxation appears through V-V and V-T/R processes. However, the V-T/R relaxation rates are expected to be very small compared with the V-V rate. Thus, the relaxation of NO was considered as through the V-V process. But, the V-T/R processes were also discussed.

Theory for V-V process

In this section we described NO+O₂ collision, and NO+N₂ collision can be described by the similar way.

Interaction Model and Potential Energy. We set up the intermolecular potential as the sum of four atom-atom interaction terms, each of which is assumed to be the Morse type:^{12,13}

$$V(\gamma_1, \gamma_2, \gamma_3, \gamma_4) = \frac{1}{4} D \sum_{i=1}^4 \left[\exp\left(-\frac{\gamma_i}{a}\right) - 2 \exp\left(\frac{l}{2} - \frac{\gamma_i}{2a}\right) \right] \quad (1)$$

Where, D , l , and a are the potential constants to be determined. For the relative separation which is significantly larger than the equilibrium bond lengths d_1 and d_2 , these atom-atom distances are approximated as

$$r_{12} = r - \gamma_1(d_1 + x_1)\cos\theta_1 \pm \frac{1}{2}(d_2 + x_2)\cos\theta_2 \quad (2a,b)$$

$$r_{34} = r + \gamma_2(d_1 + x_1)\cos\theta_1 \pm \frac{1}{2}(d_2 + x_2)\cos\theta_2 \quad (2c,d)$$

where x_i is the vibrational displacement of the i th molecule, $\gamma_1 = m_0/(m_N + m_0)$ and $\gamma_2 = m_N/(m_N + m_0)$. Here, $r_{1,2}$ are the nitrogen-oxygen distances and $r_{3,4}$ are the oxygen-oxygen distances. The relative separation between molecules 1 and 2 is denoted by r , and $\theta_1(\theta_2)$ is the angle between the direction of the intermolecular distance r and the axis of the first (second) molecule.

The present V - V energy transfer processes were considered with the energy mismatch ΔE transferred to the translational motion, i.e., a VVT mechanism. The removal of ΔE by the rotational degree of freedom is not important. The rotation, however, will certainly affect the collision dynamics, and hence, energy exchange probabilities. This effect was replaced by the rotation average. When the atom-atom distances are introduced, Eq. (1) becomes an orientation dependent function, $V(r, \theta_1, \theta_2, x_1, x_2)$, which can be averaged as

$$\bar{V}(r, x_1, x_2) = \frac{1}{4} \int_0^\pi \int_0^\pi V(r, \theta_1, \theta_2, x_1, x_2) \sin\theta_1 \sin\theta_2 d\theta_1 d\theta_2 \quad (3)$$

When the integration is performed, the orientation averaged function can be given as

$$\begin{aligned} \bar{V}(r, x_1, x_2) &\approx \left[A \exp\left(t - \frac{\gamma}{a}\right) - B \exp\left(\frac{l}{2} - \frac{r}{2a}\right) \right] \\ &+ \left[A' \exp\left(t - \frac{\gamma}{a}\right) - B' \exp\left(\frac{l}{2} - \frac{\gamma}{2a}\right) \right] \frac{x_1 x_2}{a^2} \\ &\equiv \bar{V}_0(r) + \bar{V}'(r, x_1, x_2) \end{aligned} \quad (4)$$

where

$$\begin{aligned} A &= D(a/d_2) \sinh(d_2/2a) [\sinh(Q_1)/Q_1 + \sinh(Q_2)/Q_2] \\ A' &= (D/2)(a/d_2) [\cosh(d_2/2a) - (2a/d_2) \sinh(d_2/2a)] \\ &\times (a/d_1) \{ [\cosh(Q_1) - \sinh(Q_1)/Q_1] \\ &+ [\cosh(Q_2) - \sinh(Q_2)/Q_2] \}. \end{aligned}$$

Here B is the same as $2A$ with a replaced by $2a$, and B' is the same as $A'/2$ with a also replaced by $2a$; $Q_1 = \gamma_1 d_1/a$, and $Q_2 = \gamma_2 d_2/a$. The first term \bar{V}_0 describes the relative motion of collision system, while the second term \bar{V}' is responsible for the V - V energy transfer. The collision trajectory for the present system can be determined by solving the equation of motion. When the equation of motion is solved for \bar{V}_0 , the resulting trajectory expression is¹⁴

$$\exp(l/2 - r(t)/2a) = 2E / \{ (4AE + B^2)^{1/2} \cosh[(E/2\mu)^{1/2}(t/a)] - B \}, \quad (5)$$

where E is the initial collision energy and μ is the reduced mass of the collision system. We expressed $x_1 x_2$ in terms of boson operators (a_i^+ , a_i) as $x_1 x_2 = (\hbar/2M_1\omega_1)^{1/2} (\hbar/2M_2\omega_2)^{1/2} (a_1^+ + a_1)(a_2^+ + a_2)$, where M_i and ω_i are the reduced mass and the angular frequency of molecule i , respectively. $\bar{V}'(r, x_1, x_2)$ in Eq. (4) can then be written as $\bar{V}'(r, x_1, x_2) = F(t)(a_1^+ + a_1)(a_2^+ + a_2)$. Thus, the time-dependent form of the perturbation term can be written as

$$\begin{aligned} F(t) &= \frac{\hbar}{2a^2(M_1M_2\omega_1\omega_2)^{1/2}} \left[A' \exp\left(t - \frac{\gamma(t)}{a}\right) \right. \\ &\left. - B' \exp\left(\frac{l}{2} - \frac{\gamma(t)}{2a}\right) \right] \end{aligned} \quad (6)$$

Transition Probability Expression. The Hamiltonian of the collision system can be written as

$$H(t) = \hbar\omega_1 \left(a_1^+ a_1 + \frac{1}{2} \right) + \hbar\omega_2 \left(a_2^+ a_2 + \frac{1}{2} \right) + F(t)(a_1^+ a_2 + a_1 a_2^+) \quad (7)$$

Here, the terms $a_1^+ a_2^+$ and $a_1 a_2$ was neglected, as they represent the simultaneous excitation and deexcitation of both molecules, respectively. The time evolution of the quantum state $|\psi(t)\rangle$ after collision can be determined by solving the time-dependent Schrödinger equation.

$$i\hbar |\dot{\psi}(t)\rangle = H(t) |\psi(t)\rangle \quad (8)$$

in the form^{15,16}

$$\begin{aligned} |\psi(t)\rangle &= g_0(t) \exp[g_1(t)a_1^+ a_2^+] \exp[g_2(t)a_1 a_2^+] \exp[g_3(t)a_1^+ a_1] \\ &\exp[g_4(t)a_2^+ a_2] |\psi(t_0)\rangle. \end{aligned} \quad (9)$$

To determine the time dependence of the $g_i(t)$'s, we substitute this equation in Eq. (8) and equate coefficients of the same operators on both sides. The result is

$$i\hbar \dot{g}_1(t) + F(t)g_1^2(t) + \hbar\Delta\omega g_1(t) = F(t), \quad (10a)$$

$$i\hbar \dot{g}_2(t) - 2F(t)g_1(t)g_2(t) - \hbar\Delta\omega g_2(t) = F(t), \quad (10b)$$

$$i\hbar \dot{g}_3(t) + F(t)g_3(t) = \hbar\omega_1, \quad (10c)$$

$$i\hbar \dot{g}_4(t) - F(t)g_4(t) = \hbar\omega_2. \quad (10d)$$

where $\Delta\omega = \omega_1 - \omega_2$. These equations appear in simple forms, which can be solved by standard numerical routines subject to the initial conditions $g_i(t_0) = 0$. The function $g_0(t)$ appearing

in Eq. (9) takes a simple form $g_0(t) = \exp[-\frac{1}{2}i(\omega_1 + \omega_2)t]$,

which does not appear in the probability expression derived below.

The perturbed wave function $|\psi(t)\rangle$ given in Eq. (9) contains all the information on the time evolution of the initial state $|v, 0\rangle$ and hence on the dynamics of the molecule after the perturbation is applied. In fact, we can write the perturbed wave function in the form $|\psi(t)\rangle = U(t, t_0) |\psi(t_0)\rangle$, where $U(t, t_0)$ is the time-evolution operator which, for any prescribed initial state, determines the state $|\psi(t)\rangle$. Thus the state function $|\psi(t)\rangle$ provides a complete description of the dynamics throughout the collision. For $t = t_0$, $|\psi(t_0)\rangle$ describes the initial precollision state specified beforehand for a given energy exchange process, which is $|v, 0\rangle$ in the present case. The time-evolution operator then generates various states from the initial state $|\psi(t_0)\rangle$. The probability of a $v, 0 \rightarrow v-1, 1$ transition can be found as

$$\begin{aligned} P_{v,0 \rightarrow v-1,1} &= v! (v-1)! |g_2(t)|^2 \exp[v g_3(t)]^2 \\ &\left| \sum_{n=0}^{v-1} \frac{[g_1(t)g_2(t)]^n}{n! (v-1-n)!} \right|^2 \end{aligned} \quad (11)$$

where $g_1(t)$, $g_2(t)$ and $g_3(t)$ are time-dependent solutions of Eqs. (10a)-(10c). Through the trajectory given by Eq. (5), the initial collision energy E enters in $F(t)$ and in turn enters in $g_i(t)$'s.

On the other hand, it should be noted that Eq. (11) was derived with the harmonic oscillator wave functions, but with the correct value of $\Delta E (= \hbar\Delta\omega)$ including the anharmonicity. Thus, in a rigorous calculation, it should be important to

determine the effect of the anharmonicity on energy transfer probabilities. We have, however, not considered the effect of the anharmonicity in calculation of energy transfer probabilities, because the latter is not expected to be significant.¹⁷

Rate Constant expression. Since we described the present energy transfer process with the VVT mechanism, we replaced the collision energy in Eq. (5) by the symmetrized energy $E_s = \frac{1}{4}[E_i^{\frac{1}{2}} + E_f^{\frac{1}{2}}]^2$, i.e., $E_s = \frac{1}{4}[(E \pm \Delta E)^{1/2} + E^{1/2}]^2$,

where the upper and lower signs are for exothermic and endothermic directions, respectively. Following Takayanagi's modified wave number (MWN) approximation¹⁸ we introduced the impact parameter b in the probability expression as $E(1 - b^2/r^{*2})$, where r^* is a constant distance chosen in the most important region of energy transfer. This distance will be close to the closest distance of approach in the classical head-on collision, and we can set it equal to the hard-sphere collision diameter. For large b this treatment could not be a good approximation, but the contribution of such distance collisions to energy transfer will not be important. Thus, we included $0 < b < r^*$ in this expression, assuming energy transfer is small for $\gamma > r^*$, which is an appropriate assumption for short-range interaction.^{19,20} With the introduction of the energy symmetrization and impact parameter, we obtain the average of $P_{v,0}^{-1,1}(E, b)$ over E and b as

$$P_{v,0}^{-1,1}(T) = \frac{1}{\pi r^{*2} (kT)^2} \int_0^{r^*} 2\pi b db \times \int_0^\infty E P_{v,0}^{-1,1}(E, b) \exp\left(-\frac{E}{kT}\right) dE \quad b/r^* = y \quad (12)$$

In terms of the reduced variables $E/kT = x$ and $b/r^* = y$, Eq. (12) becomes a simple expression

$$P_{v,0}^{-1,1}(T) = \int_0^1 2y dy \int_0^\infty x \exp(-x) dx P_{v,0}^{-1,1}(T; x, y) \quad (13)$$

Therefore, the calculation of $P_{v,0}^{-1,1}(T)$ does not require the absolute value of r^* . Eq. (12), or (13), is for exothermic processes. To obtain the endothermic probabilities $P(T)$, we need to evaluate the E integral from $\hbar|\Delta\omega|$. We can convert the calculated values $P_{v,0}^{-1,1}(T)$ into the rate constants as^{12,21}

$$k_{v,0}^{-1,1}(T) = Z P_{v,0}^{-1,1}(T) \\ = 4.571 \times 10^{-12} \mu^{*2} (T/\mu)^{1/2} P_{v,0}^{-1,1}(T) \text{ cm}^3/\text{molecule-sec} \quad (14)$$

where μ is the reduced mass in amu and r^* in Å. Here the rate constants have been converted from probabilities for energy transfer by multiplying the hard sphere collision frequency.

Results and Discussion

NO + O₂. The potential constants used in the calculation of energy transfer probabilities are $D(\text{NO}) = 119 \text{ k(K)}$, $D(\text{O}_2) = 113 \text{ k}$, $\sigma(\text{NO}) = 3.470 \text{ Å}$, and $\sigma(\text{O}_2) = 3.433 \text{ Å}$.²² The combining laws were used to calculate $D(\text{NO} + \text{O}_2) = 116 \text{ k}$ and $\sigma(\text{NO} + \text{O}_2) = 3.452 \text{ Å}$. The range parameter a depends weakly on temperature, but it takes a value very close to 0.20 Å ; we took the value over the temperature range.^{12,3} The dimensionless parameter l appearing in the interaction potential

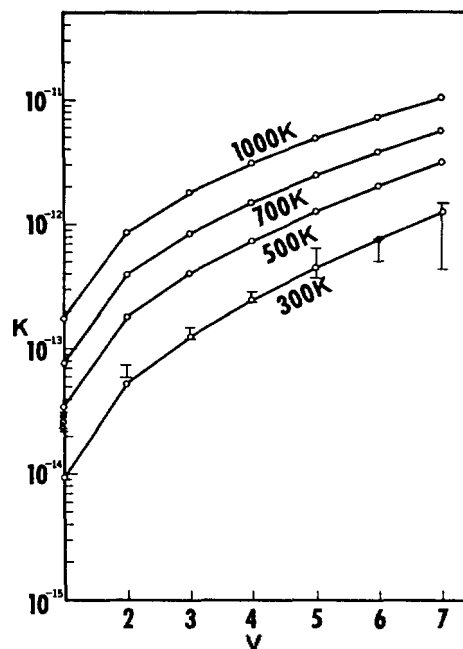


Figure 1. Energy level dependence of the calculated rate constants for $\text{NO}(v) + \text{O}_2(0) \rightarrow \text{NO}(v-1) + \text{O}_2(1)$ at four temperatures. Experimental data at 300 K: Δ ; Ref. 4, \bullet ; Ref. 6, $|$; Ref. 8, \circ ; Ref. 22.

was estimated to be $3.452/a$, where a is expressed in Å. The spectroscopic constants are $\omega_e = 1904.204$, $\omega_e x_e = 14.075$, $\omega_e y_e = 0.0077 \text{ cm}^{-1}$ for NO; $\omega_e = 1580.193$, $\omega_e x_e = 11.981$, $\omega_e y_e = 0.0475$, $\omega_e z_e = -0.00127 \text{ cm}^{-1}$ for O₂.²⁴ These were used to determine energy level spacings and the values of the energy mismatch ΔE . The equilibrium bond distances are 1.151 and 1.208 Å for NO and O₂, respectively.²⁴

In Figure 1 we presented calculated values of the V - V transition at 300, 500, 700, and 1000 K for the processes $\text{NO}(v) + \text{O}_2(0) \rightarrow \text{NO}(v-1) + \text{O}_2(1)$ from $v=1$ to 7. The calculated rate constant at 300 K increases from 9.36×10^{-15} for $v=1$ to $1.28 \times 10^{-12} \text{ cm}^3/\text{molecule-sec}$ for $v=7$. These values agree well with the experimental data obtained by Green *et al.*⁸ The experimental data^{6,8,25} for $v=1$ is, however, about two factors larger than the calculated value. That is because the electronically diabatic transitions may influence the vibrational relaxation rates.^{6,10,26} The relaxation rate constants increase also monotonically with the vibrational level v at all temperatures, and increase in direct proportion to the temperature.

The near-linear relation between $P_{v,0}^{-1,1}(T)$ and v is clearly inferred from Eq. (11). The summation term in Eq. (11), $\{1/(v-1)! + [g_1(t)g_2(t)]/(v-2)! + [g_1(t)g_2(t)]^2/2!(v-3)! + \dots\}^2$, can be reduced to $\{1/(v-1)!\}^2$, because the higher order terms from the second term are significantly less than the value of the first term. Thus, Eq. (11) can be reduced to $P_{v,0}^{-1,1} = v |g_2(t)|^2 |vg_3(t)|^2$. If $g_2(t)$ and $g_3(t)$ are the same for all v , i.e., ΔE 's for all v are the same, the probability expression given in Eq. (11) becomes $P_{v,0}^{-1,1} \sim v P_{1,0}^{0,1}$, and hence the energy transfer rate should be almost linear with v . The energy mismatch ΔE is, however, diminished from $v=1$ to $v=7$, due to the vibrational anharmonicity. Furthermore, because the energy transfer rate is in inverse proportion to

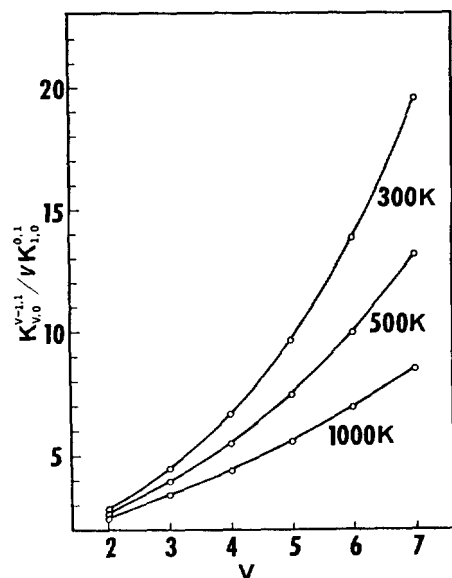


Figure 2. Scaling factors, $k_{v,0}^{v-1,1}/vk_{1,0}^{0,1}$, for $\text{NO}(v)+\text{O}_2(0)\rightarrow\text{NO}(v-1)+\text{O}_2(1)$ at three temperatures.

the energy mismatch, the increasing rates of energy transfer with v should be more than linear with v .

An important quantity for laser modeling and interpretation of much experimental work is the scaling of the rate constant with increasing vibrational states. In order to analyze this scaling we have calculated the quantity $k_{v,0}^{v-1,1}/vk_{1,0}^{0,1}$. In Figure 2 we present these scaling parameters at three different temperatures. It is known that a harmonic scaling factor would just be linear with the vibrational level v . Since we are using the harmonic oscillator wavefunction, the additional increase in higher vibrational energy level must be due to the energy correction introduced to account for the energy mismatch. In this figure, we note that the scaling factor is almost linear with the vibrational level v at higher temperature where energy mismatch becomes less important.

On the other hand, it should be noted that the experiment shows total deactivation rates (i.e., $V-V+V-T/R$) but cannot distinguish between the relative importance of $V-V$ and $V-T/R$ transfers. This information is, however, obtained from the present calculations because the theory includes two non-reactive channels without introduction of prior assumptions concerning which channel is more or less important. Because the interaction model used to derive $\bar{V}^v(r, x_1, x_2)$ in Eq. (4) can also be applied to formulate interaction potentials responsible for $V-T$ processes, we shall discuss the latter energy transfer process here. From Eq. (3), the orientation averaged perturbation energy, $\bar{V}^v(r, x_1)$, which causes this $V-T$ energy transfer, can be derived as

$$\bar{V}^v = \left[A^v \exp\left(t - \frac{\Upsilon}{a}\right) - B^v \exp\left(\frac{t}{2} - \frac{\Upsilon}{2a}\right) \right] \frac{x_1}{a}, \quad (15)$$

where

$$A^v = D(a/d_2) \sinh(d_2/2a) \\ \times (a/d_1) \{ [\cosh(Q_1) - \sinh(Q_1)/Q_1] \\ + [\cosh(Q_2) - \sinh(Q_2)/Q_2] \}.$$

B^v is the same as A^v with a replaced by $2a$. In terms of

the boson operators (a_1^+ , a_1) and the collision trajectory given in Eq. (5), this energy can be written as $V^v(r, x_1) = G(t)(a_1^+ + a_1)$. Here,

$$G(t) = \frac{1}{a} \left(\frac{\hbar}{2M_1\omega_1} \right)^{1/2} \left[A^v \exp\left(t - \frac{\Upsilon(t)}{a}\right) - B^v \exp\left(\frac{t}{2} - \frac{\Upsilon(t)}{2a}\right) \right] \quad (16)$$

For this $V-T$ process, the Hamiltonian can be written as

$$H(t) = \hbar\omega_1 \left(a_1^+ a_1 + \frac{1}{2} \right) + \hbar\omega_2 \left(a_2^+ a_2 + \frac{1}{2} \right) + G(t) (a_1^+ + a_1) \quad (17)$$

and the wave function takes the form

$$|\psi(t)\rangle = \exp[f_1(t)a_1^+] \exp[f_2(t)a_1] \exp[f_3(t)a_1^+ a_1] \\ \times \exp[f_4(t)a_2^+ a_2] \exp[f_5(t)] |\psi(t_0)\rangle. \quad (18)$$

The probability expression for the $V-T$ process $\text{NO}(v)+\text{O}_2(0)\rightarrow\text{NO}(v-1)+\text{O}_2(0)$. The probability expression for the $V-T$ process $\text{NO}(v)+\text{O}_2(0)\rightarrow\text{NO}(v-1)+\text{O}_2(0)$ then takes the form

$$P_{v,0}^{v-1,0} = v! (v-1)! |f_2(t)|^2 |\exp[vf_3(t)]|^2 \\ |\exp[f_4(t)]|^2 \times |\exp[f_5(t)]|^2 \\ \left| \sum_{n=0}^{v-1} \frac{[f_1(t)f_2(t)]^n}{n! (n+1)! (v-n-1)!} \right|^2 \quad (19)$$

In this case, $f_i(t)$'s are the solutions of the following time-dependent differential equations:

$$i\hbar\dot{f}_1(t) + \hbar\omega_1 f_1(t) = G(t), \quad (20a)$$

$$i\hbar\dot{f}_2(t) - \hbar\omega_2 f_2(t) = G(t), \quad (20b)$$

$$i\hbar\dot{f}_5(t) - G(t)f_5(t) = \frac{1}{2}(\hbar\omega_1 + \hbar\omega_2). \quad (20c)$$

The functions $f_3(t)$ and $f_4(t)$ take the simple forms $f_3(t) = \exp(-i\omega_1 t)$ and $f_4(t) = \exp(-i\omega_2 t)$, respectively. $f_1(t)$ and $f_2(t)$ can be solved by standard numerical routines, i.e., the Runge-Kutta method subject to the initial conditions $f_i(t_0) = 0$. The thermal-averaged probability, $P_{v,0}^{v-1,0}(T)$ can be also obtained by averaging $P_{v,0}^{v-1,0}(E)$ over E and b as show in Eq. (12), and converted into $k_{v,0}^{v-1,0}(T)$. The calculated rate constants for $V-T$ process are very small and can be completely negligible when calculating the relaxation of $\text{NO}(v)$ by O_2 over the temperature range of 300-1000 K. For example, the calculated $V-T$ relaxation rate constants at 300 K and 1000 K for the process $\text{NO}(1)+\text{O}_2(0)\rightarrow\text{NO}(0)+\text{O}_2(0)$, are 2.18×10^{-19} and 8.78×10^{-16} $\text{cm}^3/\text{molecule-sec}$, respectively. These values are about 5 and 2 orders of magnitude smaller than those of $V-V$, respectively. This is the case for all vibrational energy levels to $v=7$. At the same time, because the moments of inertia of NO and O_2 are so small, the $V-R$ relaxation rate constant must be the same magnitude as that of $V-T$, thus also negligible for the relaxation of $\text{NO}(v)$ by O_2 .

On the other hand, the importance of double quantum $V-V$ transition can be estimated by calculating the energy transfer rates for the process $\text{NO}(v)+\text{O}_2(0)\rightarrow\text{NO}(v-2)+\text{O}_2(2)$. The calculated values for the process $\text{NO}(2)+\text{O}_2(0)\rightarrow\text{NO}(0)+\text{O}_2(2)$ at 300 and 1000 K are 2.45×10^{-18} and 3.18×10^{-16} $\text{cm}^3/\text{molecule-sec}$, respectively. Thus, the ratios of the $\Delta v=2$

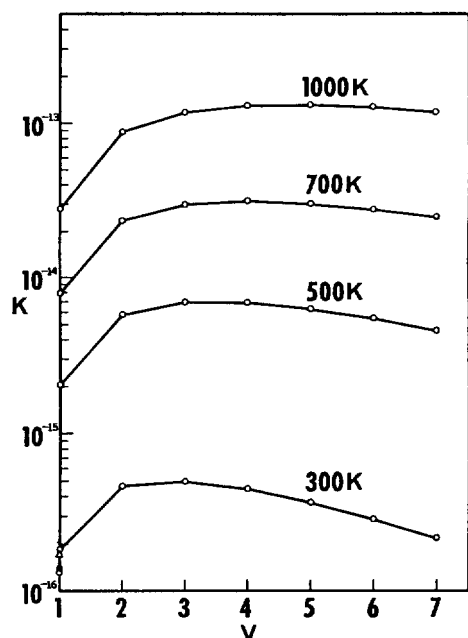


Figure 3. Energy level dependence of the calculated rate constants for $\text{NO}(v) + \text{N}_2(0) \rightarrow \text{NO}(v-1) + \text{N}_2(1)$ at four temperatures. Experimental data at 300 K: Δ ; Ref. 4, \circ ; Ref. 22, \bullet ; Ref. 24.

to $\Delta v=1$ transition are about 10^{-5} and 10^{-4} at 300 and 1000 K, respectively. For $v=7$ the ratios for the latter are about 0.002 and 0.009. Therefore, the contribution of the double quantum V-V transition as well as V-T/R transition is also negligible to the relaxation of $\text{NO}(v=1-7)$ by O_2 over the temperature range of 300-1000 K, and the relaxation can be explained completely by the single-quantum V-V transition.

NO + N₂. The potential constants are $D(\text{N}_2)=91.5$ k and $\sigma(\text{N}_2)=3.681$ Å.²² The combining laws were also used to calculate $D(\text{NO} + \text{N}_2)=104$ k and $\sigma(\text{NO} + \text{N}_2)=3.576$ Å. The dimensionless parameter l is $3.576/a$. The spectroscopic constants are $\omega_e=2358.57$, $\omega_e x_e=14.324$, $\omega_e y_e=-0.00226$, and $\omega_e z_e=-0.00024$ cm⁻¹ for N_2 .²⁴ The equilibrium bond distance for N_2 is 1.098 Å.²⁴

In Figure 3 we presented calculated values of the V-V transition at 300, 500, 700, and 1000 K for $\text{NO}(v) + \text{N}_2(0) \rightarrow \text{NO}(v-1) + \text{N}_2(1)$, for $v=1$ to $v=7$. The calculated rate constants at 300 K are 1.83×10^{-16} , 4.63×10^{-16} , 4.96×10^{-16} , 4.44×10^{-16} , 3.66×10^{-16} , 2.87×10^{-16} , and 2.18×10^{-16} cm³/molecule-sec for $v=1$ to $v=7$, respectively. These values are $3.40 \pm 1.60 \times 10^{-16}$ cm³/molecule-sec and change only slightly with the vibrational energy level v . In this figure the experimental data^{4,25,27} for $v=1$ are also presented, and agree well with the calculated data. On the other hand, both sets of data are about 2-3 orders of magnitude smaller than those for the processes $\text{NO}(v) + \text{O}_2 \rightarrow \text{NO}(v-1) + \text{O}_2$. This is because the latter are exothermic processes, while the former are endothermic. The calculated values at 500, 700, and 1000 K are also nearly independent of v . These are in the range of $6.00 \pm 1.00 \times 10^{-15}$ at 500 K, $2.70 \pm 0.40 \times 10^{-14}$ at 700 K, and $1.00 \pm 0.30 \times 10^{-13}$ cm³/molecule-sec at 1000 K except for $v=1$. The calculated values for $v=1$ over the temperature range of 500-1000 K are appreciably smaller than those for $v=2-7$.

On the other hand, the V-T/R transition and the double quantum V-V transition are also expected to contribute little to the relaxation of $\text{NO}(v)$ by N_2 , and hence, hardly effect the overall rate constant. Thus, we can conclude that the relaxation rate constants of $\text{NO}(v)$ by N_2 at all temperatures are nearly independent of the vibrational energy level v .

It is noteworthy that the relaxation rate constants of $\text{NO}(v)$ by N_2 are nearly independent of the vibrational energy level v over the entire temperature range, while those of $\text{NO}(v)$ by O_2 increase monotonically with v . If the energy mismatches ΔE 's of the process $\text{NO}(v) + \text{N}_2(0) \rightarrow \text{NO}(v-1) + \text{N}_2(1)$ for $v=1$ to $v=7$, are the same, it can also be expected that the energy transfer rates will be almost linear with v , as is the case in the process $\text{NO}(v) + \text{O}_2(0) \rightarrow \text{NO}(v-1) + \text{O}_2(1)$ through the expression $P_{v,0}^{v-1,1} \nu P_{1,0}^{0,1}$. To demonstrate this fact, we simply calculated energy transfer rates for the process $\text{NO}(v) + \text{N}_2(0) \rightarrow \text{NO}(v-1) + \text{N}_2(1)$ at 300 K for $v=1$ to $v=7$ with the same ΔE (-454 cm⁻¹ for the process $\text{NO}(1) + \text{N}_2(0) \rightarrow \text{NO}(0) + \text{N}_2(1)$). The results are 1.83×10^{-16} , 7.32×10^{-16} , 1.24×10^{-15} , 1.74×10^{-15} , 2.24×10^{-15} , 2.74×10^{-15} , and 3.24×10^{-15} cm³/molecule-sec, respectively. We notice that they are almost linear with v . But, ΔE for the latter process increases endothermically with v , due to the vibrational anharmonicity. For ΔE , they are -454 , -482 , -510 , -538 , -566 , -594 , and -622 cm⁻¹ for $v=1$ to $v=7$, respectively. Moreover, the energy transfer rate decreases as the energy mismatch increases. Thus, the decreasing effect on the energy transfer rate through the energy mismatch, counteracts the increasing effect through the probability expression, $P_{v,0}^{v-1,1} \nu P_{1,0}^{0,1}$. As a result, the relaxation rates of $\text{NO}(v)$ by N_2 become independent of v .

Concluding Comments

A semiclassical calculation of vibrational relaxation in the $\text{NO}(v=1-7) + \text{O}_2$ and $\text{NO}(v=1-7) + \text{N}_2$ collisions shows that the relaxation can be interpreted by a single-quantum V-V transition over the temperature range of 300-1000 K. The contributions of the V-T/R transition and the double quantum V-V transition are completely negligible over the entire temperature range. The vibrational relaxation rate constants for $\text{NO}(v) + \text{O}_2$ increase monotonically with the vibrational energy level v , and the scaling factor is almost linear with v at higher temperature. Those for $\text{NO}(v) + \text{N}_2$ are nearly independent of v except for $v=1$ over the entire temperature range, and are about 2-3 orders of magnitude smaller than those for $\text{NO}(v) + \text{O}_2$, because the latter is an exothermic processes while the former an endothermic.

Acknowledgement. This work was supported by the Korea Science and Engineering Foundation (KOSEF 911-0303-051-1).

References

1. X. Yang, E. H. Kim, and A. M. Wodtke, *J. Chem. Phys.*, **96**, 5111 (1992).
2. B. Seoudi, L. Doyennette, and M. Margottin-Maclou, *J. Chem. Phys.*, **81**, 5649 (1984).
3. F. A. Adel, L. Doyennette, M. Margottin-Maclou, and L. Henry, *Chem. Phys.*, **74**, 413 (1983).

4. R. E. Murphy, E. T. P. Lee, and A. M. Hart, *J. Chem. Phys.*, **63**, 2919 (1975).
5. J. C. Stephenson and S. M. Freund, *J. Chem. Phys.*, **65**, 4303 (1976).
6. R. P. Fernando and I. W. M. Smith, *J. Chem. Soc. Faraday Trans. II*, **77**, 459 (1981).
7. M. E. Whitson, Jr., L. A. Darnton, and R. J. McNeal, *Chem. Phys. Letters*, **41**, 552 (1976).
8. B. D. Green, G. E. Caledonia, R. E. Murphys, and F. X. Robert, *J. Chem. Phys.*, **76**, 2441 (1982).
9. E. E. Nikitin, *Opt. Spectry*, **9**, 8 (1960).
10. E. E. Nikitin and S. Ya. Umansky, *Faraday Discussions Chem. Soc.*, **53**, 7 (1972).
11. E. A. Andreev, S. Ya. Umansky, and A. A. Zembekov, *Chem. Phys. Letters*, **18**, 567 (1973).
12. J. Ree, C. Sohn, C. S. Lee, and Y. H. Kim, *Bull. Korean Chem. Soc.*, **8**, 449 (1987).
13. H. K. Shin, *Chem. Phys. Letters*, **64**, 21 (1979).
14. J. Ree and H. K. Shin, *Chem. Phys. Letters*, **167**, 220 (1990).
15. J. Wei and E. Norman, *J. Math. Phys.*, **4**, 575 (1963).
16. H. K. Shin, *J. Chem. Phys.*, **79**, 4285 (1983).
17. H. K. Shin, *J. Chem. Phys.*, **75**, 220 (1981).
18. K. Takayanagi, *Progr. Theoret. Phys.*, **8**, 497 (1952).
19. R. D. Sharma and C. A. Brau, *J. Chem. Phys.*, **50**, 924 (1969).
20. W. Q. Jeffers and J. D. Kelley, *J. Chem. Phys.*, **55**, 4433 (1971).
21. E. Weston, Jr. and H. A. Schwarz, *Chemical Kinetics* (Prentice-Hall Inc., Engelwood Cliffs, New Jersey, 1972) pp. 85-87.
22. J. O. Hirschfelder, C. F. Curtiss, and R. B. Bird, *Molecular Theory of Gases and Liquids* (Wiley, New York, 1964) p. 1111.
23. J. Ree and H. K. Shin, *Chem. Phys. Letters*, **163**, 308 (1989).
24. K. P. Huber and G. Herzberg, *Constants of Diatomic Molecules* (Van Nostrand Reinhold Co., New York, 1979) pp. 420, 476.
25. J. Kosanetzky, U. List, W. Urban, and H. Vormann, *Chem. Phys.*, **50**, 361 (1980).
26. K. Glänzer, *Chem. Phys.*, **22**, 367 (1977).
27. J. C. Stephenson, *J. Chem. Phys.*, **59**, 1523 (1973).

Synthesis and Configurational Analysis of Diastereomers of 5'-O-(2'-Deoxyadenosyl)-3'-O-(2'-deoxyadenosyl)-Phosphorothioate

Byung Jo Moon*, Kyung Lan Huh, and Sang Kook Kim

Department of Biochemistry, College of Natural Sciences, Kyungpook National University, Taegu 702-701. Received July 20, 1992

A procedure is described for the synthesis of the title compound *via* phosphotriester intermediates. The preparation of *R_p* and *S_p* diastereomeric dinucleotide of d[Ap(S)A] was performed by the condensation of protected deoxyadenosine, 2,5-dichlorophenylphosphorodichloridothioate and 1-hydroxybenzotriazole in THF. Their designation of configuration at phosphorus as *R_p* and *S_p* follows from analysis of ³¹P-NMR spectroscopy and reversed-phase HPLC and the stereospecificity in the hydrolysis catalyzed by nuclease P1.

Introduction

Restriction endonuclease catalyzed the cleavage of double-strand DNA specific sites. Although these enzyme are immensely important in genetic engineering, little mechanistic information is available.¹ Diastereomeric phosphorothioate analogues of nucleotides in which a nonbridging oxygen atom of a phosphate group is replaced by sulfur atom are important tools for the investigation of the stereospecificity as well as of the stereochemistry of action of these enzymes. For instance, the stereochemical course of action of EcoRI has been established by an oligonucleotide containing the appropriate recognition sequence with a phosphorothioate internucleotidic linkage of known absolute configuration.^{2,3} In a studying for mechanism of action of restriction endonuclease Hind III, we need the oligonucleotide d[Ap(s)AGCTT] which is the recognition sequence for Hind III and contains a phosphorothioate group at the cleavage site.

In this paper we described the synthesis, separation and cofigurational analysis of diastereomeric dinucleotide phosphorothioates, 5'-O-(2'-deoxyadenosyl)-3'-O-(2'-deoxyadenosyl)-phosphorothioate (d[Ap(s)A]) (Figure 1).

Result and Discussion

The desired phosphorylating agent, 2,5-dichlorophenylphosphorodichloridothioate was prepared following modifications of the reported procedure^{4,5} in 72% yield. Both diastereomers of phosphorothioate-containing d[Ap(s)A] dimer were prepared by a modification of Kemal's procedure⁶ which uses phosphotriester approach leads to high yield. The d[Ap(s)A] dimer was prepared by condensing 6-N-pivaloyl-5'-O-pixyl-2'-deoxyadenosine and 6-N-pivaloyl-3'-O-[(*p*-chlorophenoxy)acetyl]-2'-deoxyadenosine using 2,5-dichlorophenylphosphorodichloridothioate and 1-hydroxybenzotriazole as condensing agent in THF (Scheme 1). A brief treatment with ammonia